

SOUND WAVES AND SOLITONS IN HOT AND DENSE NUCLEAR MATTER

D.A. Fogaça† L.G. Ferreira Filho‡ and F.S. Navarra†

† *Instituto de Física, Universidade de São Paulo*

C.P. 66318, 05315-970 São Paulo, SP, Brazil and

‡ *Faculdade de Tecnologia, Universidade do Estado do Rio de Janeiro*

Via Dutra km 298, CEP 27523-000, Resende, RJ, Brazil

Abstract

Assuming that nuclear matter can be treated as a perfect fluid, we study the propagation of perturbations in the baryon density. The equation of state is derived from a relativistic mean field model, which is a variant of the non-linear Walecka model. The expansion of the Euler and continuity equations of relativistic hydrodynamics around equilibrium configurations leads to differential equations for the density perturbation. We solve them numerically for linear and spherical perturbations and follow the propagation of the initial pulses. For linear perturbations we find single soliton solutions and solutions with one or more solitons followed by “radiation”. Depending on the equation of state a strong damping may occur. Spherical perturbations are strongly damped and almost do not propagate. We study these equations for matter at finite temperature.

I. INTRODUCTION

Over the last decades hydrodynamics of strongly interacting systems [1, 2, 3, 4] has been applied to cold nuclear physics, to low and high energy nuclear reactions and to phenomena taking place in dense stars. Recently hydrodynamical models became more sophisticated and received more support from experimental data, in particular from the measurement of elliptic flow at RHIC [5]. Whereas other approaches can give satisfactory descriptions of the measured transverse momentum distributions, when it comes to elliptic flow, there are not many options other than hydrodynamical models. There is compelling evidence that we have seen “the perfect fluid” at RHIC. This evidence might be significantly reinforced by the observation of waves. Waves in a hadronic medium are produced in many physical situations. In fact, there are already some indications that these waves have been formed. In relativistic heavy ion collisions we may have hard parton - parton collisions in which the outgoing partons have to traverse the surrounding fluid to escape and form jets. Their passage may form Mach shock waves [6], which will affect the transverse momentum distribution of the observed final particles. These “Mach cones” may have been observed at RHIC [7, 8].

Under certain conditions waves may form solitons. Therefore we can go a step further and look for solitons in a hadronic medium. In the RHIC scenario, for example, the same supersonic motion that generates conical shock waves may also generate solitons. Whether or not this happens, depends on details of the equation of state and on the approximations used in the hydrodynamical description of the motion. Another scenario where solitons may appear is in the core of dense stars. Here perturbations in the baryon density may be caused, for example, by interactions of neutrinos with the baryonic matter. In a pioneering series of works on soliton formation in nuclear matter [9, 10, 11] it was suggested that in nucleon - nucleus collision at intermediate bombarding energies ($\simeq 50 - 200$ MeV) the nucleon may be absorbed by the nucleus (treated as a fluid at rest) and propagate as a localized pulse of baryon density.

In this work we study the propagation of sound waves in dense and hot hadronic matter. More specifically we consider the propagation of perturbations in the baryon density. These perturbations may generate ordinary waves, shock waves and also Korteweg - de Vries (KdV) solitons. Starting from the equations of relativistic hydrodynamics at zero and finite temperature and in Cartesian (x, t) and spherical (r, θ, ϕ, t) coordinates, we derive differen-

tial equations and find their numerical solutions. The equation of state is derived from a relativistic mean field model of the Walecka type [12, 13, 14]. We discuss the features of the solutions and the role played by the microscopic interactions in the shape and propagation of the sound waves.

In a previous work [15] we have studied the formation and propagation of KdV solitons in cold nuclear matter. We found that these solitary waves can indeed exist in the nuclear medium, provided that derivative couplings between the nucleon and the vector field are included in the interaction Lagrangian. For this class of equation of state (EOS), which is quite general, perturbations on the nuclear density can propagate as a pulse without dissipation.

During the analysis of several realistic nuclear equations of state, we realized that, very often the speed of sound c_s is in the range 0.15 – 0.25. Compared to the speed of light these values are not large but not very small either. This suggests that, even for slowly moving nuclear matter, relativistic effects might be sizeable. We investigated these effects in [16] and in [17].

The propagation of density pulses might be relevant for the astrophysics of dense stars. This motivated us to extend our results to the spherical geometry. In [18] combining the Euler and continuity equations in relativistic hydrodynamics in spherical coordinates, we have obtained for the first time an equation similar to the KdV equation. Spherical KdV - like equations have been found before in other contexts, as, for example, in the study of nonlinear waves in dusty plasmas [19, 20].

In the present work we reexamine all our previous works, looking for the numerical solutions of the previously encountered differential equations. In the linear case we compare the analytical solution with the numerical one and study the sensitivity of the solution to the initial conditions. In the spherical case there is no analytical solution. Our numerical solution could be compared to the one found in [19, 20]. We have extended the formalism to finite temperature and, with the new equation of state, derived differential equations which are temperature dependent. We have also studied the limiting case where the differential equations generate shock waves.

The text is organized as follows. In section II, for convenience, we collect some useful formulas for hydrodynamics. In section III we present the equation of state obtained with our model. In sections IV we derive the spherical KdV-like equations and in section V we

present and discuss the numerical solutions of these equations. Finally, in section VI we present some conclusions.

II. RELATIVISTIC HYDRODYNAMICS

In this section we review the main equations of relativistic hydrodynamics. In natural units ($c = 1$) the velocity four vector u^ν is defined as:

$$u^\nu = (u^0, \vec{u}) = (\gamma, \gamma\vec{v}) \quad (1)$$

where γ is the Lorentz contraction factor given by $\gamma = (1 - v^2)^{-1/2}$. The velocity field of matter is $\vec{v} = \vec{v}(t, x, y, z)$ and thus $u^\nu u_\nu = 1$. The energy-momentum tensor is, as usual, given by:

$$T_{\mu\nu} = (\varepsilon + p)u_\mu u_\nu - pg_{\mu\nu} \quad (2)$$

where ε and p are the energy density and pressure respectively ($g_{00} = -g_{ii} = 1$ and $g_{\mu\nu} = 0$ if $\mu \neq \nu$). Energy-momentum conservation is ensured by:

$$\partial_\nu T_\mu{}^\nu = 0 \quad (3)$$

The projection of (3) onto a direction perpendicular to u^μ gives us the relativistic version of Euler equation [21, 22, 23]:

$$\frac{\partial \vec{v}}{\partial t} + (\vec{v} \cdot \vec{\nabla})\vec{v} = -\frac{1}{(\varepsilon + p)\gamma^2} \left(\vec{\nabla} p + \vec{v} \frac{\partial p}{\partial t} \right) \quad (4)$$

The continuity equation for the baryon number is [21, 22, 23]:

$$\partial_\nu j_B{}^\nu = 0 \quad (5)$$

Since $j_B{}^\nu = u^\nu \rho_B$, where ρ_B is the baryon density, the above equation reads

$$\frac{\partial}{\partial t}(\rho_B \gamma) + \vec{\nabla} \cdot (\rho_B \gamma \vec{v}) = 0 \quad (6)$$

or

$$\frac{\partial \rho_B}{\partial t} + \gamma^2 v \rho_B \left(\frac{\partial v}{\partial t} + \vec{v} \cdot \vec{\nabla} v \right) + \vec{\nabla} \cdot (\rho_B \vec{v}) = 0 \quad (7)$$

The enthalpy per nucleon is given by [22]:

$$dh = T ds + V dp \quad (8)$$

where $V = 1/\rho_B$ is the specific volume. T and s are the temperature and entropy density respectively. For a perfect fluid ($ds = 0$) the equation above becomes $dp = \rho_B dh$ and consequently:

$$\vec{\nabla}p = \rho_B \vec{\nabla}h, \quad \frac{\partial p}{\partial t} = \rho_B \frac{\partial h}{\partial t} \quad (9)$$

The Gibbs relation is [24]:

$$\varepsilon + p = \mu_B \rho_B + Ts \quad (10)$$

where μ_B is the baryochemical potential. Inserting (9) and (10) in (4) we find:

$$\frac{\partial \vec{v}}{\partial t} + (\vec{v} \cdot \vec{\nabla})\vec{v} = -\frac{\rho_B}{(\mu_B \rho_B + Ts)\gamma^2} \left(\vec{\nabla}h + \vec{v} \frac{\partial h}{\partial t} \right) \quad (11)$$

The enthalpy per nucleon can also be calculated with the expression [11]:

$$h = E + \rho_B \frac{\partial E}{\partial \rho_B} \quad (12)$$

where E is the energy per nucleon given by:

$$E = \frac{\varepsilon}{\rho_B}$$

which, inserted into (12) yields:

$$h = \frac{\partial \varepsilon}{\partial \rho_B} \quad (13)$$

It is clear that the ‘‘force’’ on the right hand side of (11) will be ultimately determined by the equation of state, i.e., by the function $\varepsilon(\rho_B)$.

III. EQUATION OF STATE

Equation (11) contains the gradient of the derivative of the energy density. If ε contains a Laplacian of ρ_B , i.e., $\varepsilon \propto \dots + \dots \nabla^2 \rho_B + \dots$, then (11) will have a cubic derivative with respect to the space coordinate, which will give rise to the Korteweg-de Vries equation for the baryon density. The most popular relativistic mean field models do not have higher derivative terms and, even if they have at the start, these terms are usually neglected during the calculations.

As in [15] we shall use a variant of the non-linear Walecka model [12] given by:

$$\mathcal{L} = \mathcal{L}_{QHD} + \frac{dg_V}{m_V^2} \bar{\psi} (\partial_\nu \partial^\nu V_\mu) \gamma^\mu \psi \quad (14)$$

with

$$\begin{aligned} \mathcal{L}_{QHD} = & \bar{\psi}[\gamma_\mu(i\partial^\mu - g_V V^\mu) - (M - g_S\phi)]\psi + \frac{1}{2}(\partial_\mu\phi\partial^\mu\phi - m_S^2\phi^2) + \\ & -\frac{b\phi^3}{3} - \frac{c\phi^4}{4} - \frac{1}{4}F_{\mu\nu}F^{\mu\nu} + \frac{1}{2}m_V^2V_\mu V^\mu \end{aligned}$$

where $F_{\mu\nu} = \partial_\mu V_\nu - \partial_\nu V_\mu$. As usual, the degrees of freedom are the baryon field ψ , the neutral scalar meson field ϕ and the neutral vector meson field V_μ , with the respective couplings and masses. The second and new term in (14) is designed to be small in comparison with the main baryon - vector meson interaction term $g_V\bar{\psi}\gamma_\mu V^\mu\psi$. Because of the derivatives, it is of the order of:

$$\frac{p^2}{m_V^2} \sim \frac{k_F^2}{m_V^2} \sim 0.12 \quad (15)$$

where the Fermi momentum is $k_F \simeq 0.28$ GeV and $m_V \simeq 0.8$ GeV. The form chosen for the new interaction term is not dictated by any symmetry argument, has no other deep justification and is just one possible interaction term among many others. It is used here as a prototype. At this stage our main interest is to explore the effects of these higher derivative terms, which may generate more complex wave equations. The parameter d is free and will act as a ‘‘marker’’. Setting d equal to zero will switch off the new term. On the other hand $d = 1$ means that the coupling g_V is the standard one. Other values imply a correction in this coupling.

The mean field approximation means that $V_\mu \rightarrow \langle V_\mu \rangle \equiv \delta_{\mu 0}V_0$ and $\phi \rightarrow \langle \phi \rangle \equiv \phi_0$. With the above Lagrangian and the corresponding Hamiltonian we can, following the standard procedure, write the partition function of the system and calculate the energy density, the pressure and entropy density, which, for symmetric nuclear matter, are given by [25]:

$$\begin{aligned} \varepsilon = & \frac{b}{3g_S^3}(M - M^*)^3 + \frac{c}{4g_S^4}(M - M^*)^4 + \frac{\gamma_s}{(2\pi)^3} \int d^3k h_+ [n_{\vec{k}}(T, \nu) + \bar{n}_{\vec{k}}(T, \nu)] \\ & + \frac{g_V^2}{2m_V^2}\rho_B^2 + \frac{m_S^2}{2g_S^2}(M - M^*)^2 + \frac{d g_V^2}{m_V^4}\rho_B \vec{\nabla}^2 \rho_B - \frac{d g_V^2}{m_V^4}\rho_B \left(\frac{\partial^2 \rho_B}{\partial t^2} \right) \end{aligned} \quad (16)$$

$$\begin{aligned} p = & \frac{g_V^2}{2m_V^2}\rho_B^2 - \frac{m_S^2}{2g_S^2}(M - M^*)^2 - \frac{b}{3g_S^3}(M - M^*)^3 - \frac{c}{4g_S^4}(M - M^*)^4 \\ & - T \frac{\gamma_s}{(2\pi)^3} \int d^3k \left\{ \ln[(1 - n_{\vec{k}}(T, \nu))] + \ln[(1 - \bar{n}_{\vec{k}}(T, \nu))] \right\} \\ & - \frac{d g_V^2}{m_V^4}\rho_B \vec{\nabla}^2 \rho_B + \frac{d g_V^2}{m_V^4}\rho_B \left(\frac{\partial^2 \rho_B}{\partial t^2} \right) \end{aligned} \quad (17)$$

and

$$s = -\frac{\gamma_s}{(2\pi)^3} \int d^3k \left\{ n_{\vec{k}}(T, \nu) \ln [n_{\vec{k}}(T, \nu)] + [1 - n_{\vec{k}}(T, \nu)] \ln [1 - n_{\vec{k}}(T, \nu)] + \right. \\ \left. + \bar{n}_{\vec{k}}(T, \nu) \ln [\bar{n}_{\vec{k}}(T, \nu)] + [1 - \bar{n}_{\vec{k}}(T, \nu)] \ln [1 - \bar{n}_{\vec{k}}(T, \nu)] \right\} \quad (18)$$

where $\gamma_s = 4$ is the degeneracy factor and M^* is the effective nucleon mass ($M^* = M - g_S \phi_0$) given by:

$$M^* = M - \frac{g_S^2}{m_S^2} \frac{\gamma_s}{(2\pi)^3} \int d^3k \frac{M^*}{h_+} [n_{\vec{k}}(T, \nu) + \bar{n}_{\vec{k}}(T, \nu)] + \\ + \frac{g_S^2}{m_S^2} \left[\frac{b}{g_S^3} (M - M^*)^2 + \frac{c}{g_S^4} (M - M^*)^3 \right] \quad (19)$$

and

$$\rho_B = \frac{\gamma_s}{(2\pi)^3} \int d^3k [n_{\vec{k}}(T, \nu) - \bar{n}_{\vec{k}}(T, \nu)] \quad (20)$$

with

$$n_{\vec{k}}(T, \nu) \equiv \frac{1}{1 + e^{(h_+ - \nu)/T}} \quad (21)$$

$$\bar{n}_{\vec{k}}(T, \nu) \equiv \frac{1}{1 + e^{(h_+ + \nu)/T}} \quad (22)$$

$$\nu \equiv \mu_B - g_V V_0 \quad (23)$$

$$h_+ \equiv (\vec{k}^2 + M^{*2})^{1/2} \quad (24)$$

The last two terms of (16) come from the new interaction term in (14). Baryon number propagation in nuclear matter has been studied in [26] with the help of the diffusion equation:

$$\frac{\partial \rho_B}{\partial t} = D \nabla^2 \rho_B \quad (25)$$

where the diffusion constant D was numerically evaluated as a function of density and temperature and found to be $D \simeq 0.35 fm$ at densities comparable to the equilibrium nuclear density and temperatures of the order of 80 MeV. This number is small compared to any nuclear size scale and can be interpreted as indicating that density gradients do not disappear very rapidly in nuclear matter. Using (25) twice in the last term of (16) it can be rewritten as:

$$-\frac{d g_V^2}{m_V^4} \rho_B \left(\frac{\partial^2 \rho_B}{\partial t^2} \right) = -\frac{d g_V^2}{m_V^4} \rho_B \frac{\partial}{\partial t} \left(D \nabla^2 \rho_B \right) = -\frac{d g_V^2}{m_V^4} \rho_B D^2 [\nabla^2 (\nabla^2 \rho_B)] \quad (26)$$

which, in the context of the present calculation, can be neglected because $\nabla^2 (\nabla^2 \rho_B) \ll (\nabla^2 \rho_B)$. With this last approximation, the final form of the energy density is given by (16)

without the last term. Of course, the same argument holds for the pressure, which will be given by (17) without the last term.

When $T = 0$ the energy density reduces to:

$$\begin{aligned} \varepsilon = & \frac{g_V^2}{2m_V^2} \rho_B^2 + \frac{m_S^2}{2g_S^2} (M - M^*)^2 + \frac{d g_V^2}{m_V^4} \rho_B \vec{\nabla}^2 \rho_B + \frac{b}{3g_S^3} (M - M^*)^3 + \\ & + \frac{c}{4g_S^4} (M - M^*)^4 + \frac{\gamma_s}{(2\pi)^3} \int_0^{k_F} d^3k h_+ \end{aligned} \quad (27)$$

From (16) + (17) we can check that the Gibbs relation (10) is fulfilled. The speed of sound c_s is given by:

$$c_s^2 = \frac{\partial p}{\partial \varepsilon} \quad (28)$$

The numerical inputs for the above formulas for $T = 0$ were taken from [12] and are shown in Table I. In the Table the incompressibility K , the effective nucleon mass M^* , the speed of sound c_s and the saturation density ρ_0 are calculated. For $T > 0$ the sign of the parameter c is reversed. In order to test our routines we have reproduced the results shown in Table I, but in what follows all the results will be obtained with the parameter set NL1.

	<i>QHD</i>	<i>NL1</i>	<i>NL3</i>	<i>NL3 - II</i>	<i>NL - SH</i>
K(MeV)	545	211	272	272	355
M(MeV)	939	938	939	939	939
m_S (MeV)	500	492	508,2	507,7	526
m_V (MeV)	780	783	782,5	781,9	783
g_S	8,7	10,14	10,22	10,2	10,4
g_V	11,62	13,28	12,87	12,8	12,9
M^*/M	0,56	0,57	0,6	0,59	0,6
ρ_0 (fm^{-3})	0,19	0,15	0,15	0,15	0,15
b (fm^{-1})	0	+12,17	+10,43	+10,4	+6,9
c	0	-36,26	-28,9	-28,9	-15,8
c_s	0,25	0,16	0,18	0,18	0,2

Table I: Numerical inputs [12] for the equation of state. K , M^* , ρ_0 and c_s are calculated.

IV. DERIVATION OF THE SPHERICAL KDV EQUATION

A. Zero temperature

This section contains the derivation of the spherical KdV equation. The general scheme is the same as the one used in [15] for the one dimensional Cartesian problem. However, as it will be seen, there are new details, which deserve the discussion presented below. We shall be concerned only with problems which have spherical symmetry. Therefore the continuity equation (7) and Euler equation (11) will have only radial components and the derivatives with respect to angles will vanish.

Cold nuclear matter exhibits the saturation property, i.e., the energy per nucleon as a function of the baryon density ($E = \varepsilon/\rho_B$) has a minimum. Thus we start with (27) and impose the saturation condition:

$$\frac{\partial}{\partial \rho_B} \left(\frac{\varepsilon}{\rho_B} - M \right)_{\rho_B = \rho_0} = 0 \quad (29)$$

We then perform a Taylor expansion of E around the equilibrium density ρ_0 up to second order:

$$E(\rho_B) = E(\rho_0) + \frac{1}{2} \left(\frac{\partial^2 E}{\partial \rho_B^2} \right)_{\rho_B = \rho_0} (\rho_B - \rho_0)^2 \quad (30)$$

As in [11], the density ρ_B and its gradient $\vec{\nabla} \rho_B$ are treated as independent variables. Inserting the above expression into (12) and using the relation [11]

$$\left(\frac{\partial^2 E}{\partial \rho_B^2} \right)_{\rho_B = \rho_0} = \frac{M c_s^2}{\rho_0^2} \quad (31)$$

we obtain:

$$\begin{aligned} h = & \frac{g_V^2}{2m_V^2} \rho_0 + \frac{m_S^2}{2\rho_0} \left[\frac{(M^* - M)}{g_S} \right]^2 + \frac{\gamma_s}{(2\pi)^3 \rho_0} \int_0^{k_F} d^3 k (k^2 + M^{*2})^{1/2} + \\ & + \frac{b}{3g_S^3 \rho_0} (M - M^*)^3 + \frac{c}{4g_S^4 \rho_0} (M - M^*)^4 + d \frac{g_V^2}{m_V^4} \vec{\nabla}^2 \rho_B + \\ & + \frac{M c_s^2}{2\rho_0^2} (3\rho_B^2 - 4\rho_B \rho_0 + \rho_0^2) \end{aligned} \quad (32)$$

With the above expression we compute the derivatives:

$$\frac{\partial h}{\partial r} = -\frac{2M c_s^2}{\rho_0} \frac{\partial \rho_B}{\partial r} + \frac{3M c_s^2}{\rho_0^2} \rho_B \frac{\partial \rho_B}{\partial r} + d \frac{g_V^2}{m_V^4} \frac{\partial^3 \rho_B}{\partial r^3} +$$

$$+ d \frac{g_V^2}{m_V^4} \frac{2}{r} \frac{\partial^2 \rho_B}{\partial r^2} - d \frac{g_V^2}{m_V^4} \frac{2}{r^2} \frac{\partial \rho_B}{\partial r} \quad (33)$$

and also:

$$\begin{aligned} \frac{\partial h}{\partial t} = & -\frac{2Mc_s^2}{\rho_0} \frac{\partial \rho_B}{\partial t} + \frac{3Mc_s^2}{\rho_0^2} \rho_B \frac{\partial \rho_B}{\partial t} + d \frac{g_V^2}{m_V^4} \frac{\partial}{\partial t} \left(\frac{\partial^2 \rho_B}{\partial r^2} \right) + \\ & + d \frac{g_V^2}{m_V^4} \frac{2}{r} \frac{\partial}{\partial t} \left(\frac{\partial \rho_B}{\partial r} \right) - d \frac{g_V^2}{m_V^4} \frac{2v}{r^2} \frac{\partial \rho_B}{\partial r} \end{aligned} \quad (34)$$

Inserting (33) and (34) into (11) we find:

$$\begin{aligned} \frac{\partial v}{\partial t} + v \frac{\partial v}{\partial r} = & \frac{(v^2 - 1)}{\mu_B} \left\{ \left(\frac{3Mc_s^2}{\rho_0^2} \rho_B - \frac{2Mc_s^2}{\rho_0} \right) \left(\frac{\partial \rho_B}{\partial r} + v \frac{\partial \rho_B}{\partial t} \right) + d \frac{g_V^2}{m_V^4} \left[\frac{\partial^3 \rho_B}{\partial r^3} + v \frac{\partial}{\partial t} \left(\frac{\partial^2 \rho_B}{\partial r^2} \right) \right] + \right. \\ & \left. + d \frac{2g_V^2}{rm_V^4} \left[\frac{\partial^2 \rho_B}{\partial r^2} - \frac{1}{r} \frac{\partial \rho_B}{\partial r} + v \frac{\partial}{\partial t} \left(\frac{\partial \rho_B}{\partial r} \right) - \frac{v^2}{r} \frac{\partial \rho_B}{\partial r} \right] \right\} \end{aligned} \quad (35)$$

We now rewrite (35) e (7) in terms of the dimensionless variables:

$$\hat{\rho} = \frac{\rho_B}{\rho_0} , \quad \hat{v} = \frac{v}{c_s} \quad (36)$$

where ρ_0 is the equilibrium baryon density given in Table I and c_s is the speed of sound.

The Euler equation becomes:

$$\begin{aligned} c_s \frac{\partial \hat{v}}{\partial t} + c_s^2 \hat{v} \frac{\partial \hat{v}}{\partial r} = & \frac{(c_s^2 \hat{v}^2 - 1)}{\mu_B} \left\{ \left(\frac{3Mc_s^2}{\rho_0^2} \rho_0 \hat{\rho} - \frac{2Mc_s^2}{\rho_0} \right) \rho_0 \left(\frac{\partial \hat{\rho}}{\partial r} + c_s \hat{v} \frac{\partial \hat{\rho}}{\partial t} \right) + d \frac{g_V^2}{m_V^4} \rho_0 \left[\frac{\partial^3 \hat{\rho}}{\partial r^3} + \right. \right. \\ & \left. \left. c_s \hat{v} \frac{\partial}{\partial t} \left(\frac{\partial^2 \hat{\rho}}{\partial r^2} \right) \right] + d \frac{2g_V^2}{rm_V^4} \rho_0 \left[\frac{\partial^2 \hat{\rho}}{\partial r^2} - \frac{1}{r} \frac{\partial \hat{\rho}}{\partial r} + c_s \hat{v} \frac{\partial}{\partial t} \left(\frac{\partial \hat{\rho}}{\partial r} \right) - \frac{c_s^2 \hat{v}^2}{r} \frac{\partial \hat{\rho}}{\partial r} \right] \right\} \end{aligned} \quad (37)$$

and the continuity equation becomes:

$$(1 - c_s^2 \hat{v}^2) \left(\frac{\partial \hat{\rho}}{\partial t} + c_s \hat{\rho} \frac{\partial \hat{v}}{\partial r} + c_s \hat{v} \frac{\partial \hat{\rho}}{\partial r} + \frac{2c_s \hat{\rho} \hat{v}}{r} \right) + c_s^2 \hat{\rho} \hat{v} \left(\frac{\partial \hat{v}}{\partial t} + c_s \hat{v} \frac{\partial \hat{v}}{\partial r} \right) = 0 \quad (38)$$

We next define the “stretched coordinates” ξ and τ as in [9, 10, 11, 27]:

$$\xi = \sigma^{1/2} \frac{(r - c_s t)}{R} , \quad \tau = \sigma^{3/2} \frac{c_s t}{R} \quad (39)$$

where R is a size scale and σ is a small ($0 < \sigma < 1$) expansion parameter. The derivatives become the following operators:

$$\begin{aligned} \frac{\partial}{\partial r} = & \frac{\sigma^{1/2}}{R} \frac{\partial}{\partial \xi} , \quad \frac{\partial^2}{\partial r^2} = \frac{\sigma}{R^2} \frac{\partial^2}{\partial \xi^2} , \quad \frac{\partial^3}{\partial r^3} = \frac{\sigma^{3/2}}{R^3} \frac{\partial^3}{\partial \xi^3} \quad \text{and} \\ \frac{\partial}{\partial t} = & -\frac{\sigma^{1/2} c_s}{R} \frac{\partial}{\partial \xi} + \frac{\sigma^{3/2} c_s}{R} \frac{\partial}{\partial \tau} \end{aligned} \quad (40)$$

From (39) we can see that:

$$r = \frac{R\xi\sigma + R\tau}{\sigma^{3/2}} \quad (41)$$

and thus:

$$\frac{1}{r^2} = \frac{\sigma^3}{(R\xi\sigma + R\tau)^2} \quad (42)$$

In the $\xi - \tau$ space (37) reads:

$$\begin{aligned} & -\frac{\sigma^{1/2}c_s^2}{R}\frac{\partial\hat{v}}{\partial\xi} + \frac{\sigma^{3/2}c_s^2}{R}\frac{\partial\hat{v}}{\partial\tau} + c_s^2\frac{\sigma^{1/2}}{R}\hat{v}\frac{\partial\hat{v}}{\partial\xi} = \\ & = \frac{(c_s^2\hat{v}^2 - 1)}{\mu_B} \left\{ \left(\frac{3Mc_s^2}{\rho_0^2}\rho_0\hat{\rho} - \frac{2Mc_s^2}{\rho_0} \right) \rho_0 \left(\frac{\sigma^{1/2}}{R}\frac{\partial\hat{\rho}}{\partial\xi} - \frac{\sigma^{1/2}c_s^2}{R}\hat{v}\frac{\partial\hat{\rho}}{\partial\xi} + \frac{\sigma^{3/2}c_s^2}{R}\hat{v}\frac{\partial\hat{\rho}}{\partial\tau} \right) + \right. \\ & \quad + d\frac{g_V^2}{m_V^4}\rho_0 \left[\frac{\sigma^{3/2}}{R^3}\frac{\partial^3\hat{\rho}}{\partial\xi^3} + \left(-\frac{\sigma^{1/2}c_s^2}{R}\hat{v}\frac{\partial}{\partial\xi} + \frac{\sigma^{3/2}c_s^2}{R}\hat{v}\frac{\partial}{\partial\tau} \right) \left(\frac{\sigma}{R^2}\frac{\partial^2\hat{\rho}}{\partial\xi^2} \right) \right] + \\ & \quad + d\frac{2g_V^2\rho_0\sigma^{3/2}}{m_V^4(R\xi\sigma + R\tau)} \left[\frac{\sigma}{R^2}\frac{\partial^2\hat{\rho}}{\partial\xi^2} - \frac{\sigma^{3/2}}{(R\xi\sigma + R\tau)}\frac{\sigma^{1/2}}{R}\frac{\partial\hat{\rho}}{\partial\xi} + \right. \\ & \quad \left. \left. + c_s\hat{v} \left(-\frac{\sigma^{1/2}c_s}{R}\frac{\partial}{\partial\xi} + \frac{\sigma^{3/2}c_s}{R}\frac{\partial}{\partial\tau} \right) \left(\frac{\sigma^{1/2}}{R}\frac{\partial\hat{\rho}}{\partial\xi} \right) - \frac{c_s^2\hat{v}^2\sigma^{3/2}}{(R\xi\sigma + R\tau)}\frac{\sigma^{1/2}}{R}\frac{\partial\hat{\rho}}{\partial\xi} \right] \right\} \quad (43) \end{aligned}$$

and the continuity equation (38) reads:

$$\begin{aligned} & (1 - c_s^2\hat{v}^2) \left(-\frac{\sigma^{1/2}c_s}{R}\frac{\partial\hat{\rho}}{\partial\xi} + \frac{\sigma^{3/2}c_s}{R}\frac{\partial\hat{\rho}}{\partial\tau} + c_s\hat{\rho}\frac{\sigma^{1/2}}{R}\frac{\partial\hat{v}}{\partial\xi} + c_s\hat{v}\frac{\sigma^{1/2}}{R}\frac{\partial\hat{\rho}}{\partial\xi} + \frac{2c_s\hat{\rho}\hat{v}\sigma^{3/2}}{(R\xi\sigma + R\tau)} \right) + \\ & \quad + c_s^2\hat{\rho}\hat{v} \left(-\frac{\sigma^{1/2}c_s}{R}\frac{\partial\hat{v}}{\partial\xi} + \frac{\sigma^{3/2}c_s}{R}\frac{\partial\hat{v}}{\partial\tau} + c_s\hat{v}\frac{\sigma^{1/2}}{R}\frac{\partial\hat{v}}{\partial\xi} \right) = 0 \quad (44) \end{aligned}$$

We then expand (36) around the equilibrium values:

$$\hat{\rho} = 1 + \sigma\rho_1 + \sigma^2\rho_2 + \dots = 1 + \hat{\rho}_1 + \hat{\rho}_2 + \dots \quad (45)$$

$$\hat{v} = \sigma v_1 + \sigma^2 v_2 + \dots \quad (46)$$

With this expansion (43) becomes:

$$\begin{aligned} & -\frac{\sigma^{1/2}c_s^2}{R}\frac{\partial}{\partial\xi}(\sigma v_1 + \sigma^2 v_2 + \dots) + \frac{\sigma^{3/2}c_s^2}{R}\frac{\partial}{\partial\tau}(\sigma v_1 + \sigma^2 v_2 + \dots) + \\ & \quad + c_s^2\frac{\sigma^{1/2}}{R}(\sigma v_1 + \sigma^2 v_2 + \dots)\frac{\partial}{\partial\xi}(\sigma v_1 + \sigma^2 v_2 + \dots) = \\ & \quad = \frac{[c_s^2(\sigma v_1 + \sigma^2 v_2 + \dots)^2 - 1]}{\mu_B} \times \\ & \quad \times \left\{ \left[\frac{3Mc_s^2}{\rho_0^2}\rho_0(1 + \sigma\rho_1 + \sigma^2\rho_2 + \dots) - \frac{2Mc_s^2}{\rho_0} \right] \rho_0 \left[\frac{\sigma^{1/2}}{R}\frac{\partial}{\partial\xi}(1 + \sigma\rho_1 + \sigma^2\rho_2 + \dots) + \right. \right. \end{aligned}$$

$$\begin{aligned}
& -\frac{\sigma^{1/2}c_s^2}{R}(\sigma v_1 + \sigma^2 v_2 + \dots) \frac{\partial}{\partial \xi} (1 + \sigma \rho_1 + \sigma^2 \rho_2 + \dots) + \\
& + \frac{\sigma^{3/2}c_s^2}{R}(\sigma v_1 + \sigma^2 v_2 + \dots) \frac{\partial}{\partial \tau} (1 + \sigma \rho_1 + \sigma^2 \rho_2 + \dots) \Big] + \\
& + d \frac{g_V^2}{m_V^4} \rho_0 \left[\frac{\sigma^{3/2}}{R^3} \frac{\partial^3}{\partial \xi^3} (1 + \sigma \rho_1 + \sigma^2 \rho_2 + \dots) + \left(-\frac{\sigma^{1/2}c_s^2}{R}(\sigma v_1 + \sigma^2 v_2 + \dots) \frac{\partial}{\partial \xi} + \right. \right. \\
& \left. \left. + \frac{\sigma^{3/2}c_s^2}{R}(\sigma v_1 + \sigma^2 v_2 + \dots) \frac{\partial}{\partial \tau} \right) \left(\frac{\sigma}{R^2} \frac{\partial^2}{\partial \xi^2} (1 + \sigma \rho_1 + \sigma^2 \rho_2 + \dots) \right) \right] + \\
& + d \frac{2g_V^2 \rho_0 \sigma^{3/2}}{m_V^4 (R\xi\sigma + R\tau)} \left[\frac{\sigma}{R^2} \frac{\partial^2}{\partial \xi^2} (1 + \sigma \rho_1 + \sigma^2 \rho_2 + \dots) + \right. \\
& \left. - \frac{\sigma^{3/2}}{(R\xi\sigma + R\tau)} \frac{\sigma^{1/2}}{R} \frac{\partial}{\partial \xi} (1 + \sigma \rho_1 + \sigma^2 \rho_2 + \dots) + \right. \\
& \left. + c_s (\sigma v_1 + \sigma^2 v_2 + \dots) \left(-\frac{\sigma^{1/2}c_s}{R} \frac{\partial}{\partial \xi} + \frac{\sigma^{3/2}c_s}{R} \frac{\partial}{\partial \tau} \right) \left(\frac{\sigma^{1/2}}{R} \frac{\partial}{\partial \xi} (1 + \sigma \rho_1 + \sigma^2 \rho_2 + \dots) \right) \right. \\
& \left. - \frac{c_s^2 (\sigma v_1 + \sigma^2 v_2 + \dots)^2 \sigma^{3/2}}{(R\xi\sigma + R\tau)} \frac{\sigma^{1/2}}{R} \frac{\partial}{\partial \xi} (1 + \sigma \rho_1 + \sigma^2 \rho_2 + \dots) \right] \Big\} \quad (47)
\end{aligned}$$

and (44) becomes:

$$\begin{aligned}
& [1 - c_s^2 (\sigma v_1 + \sigma^2 v_2 + \dots)^2] \left(-\frac{\sigma^{1/2}c_s}{R} \frac{\partial}{\partial \xi} (1 + \sigma \rho_1 + \sigma^2 \rho_2 + \dots) + \right. \\
& \left. + \frac{\sigma^{3/2}c_s}{R} \frac{\partial}{\partial \tau} (1 + \sigma \rho_1 + \sigma^2 \rho_2 + \dots) + \right. \\
& \left. + c_s (1 + \sigma \rho_1 + \sigma^2 \rho_2 + \dots) \frac{\sigma^{1/2}}{R} \frac{\partial}{\partial \xi} (\sigma v_1 + \sigma^2 v_2 + \dots) + \right. \\
& \left. + c_s (\sigma v_1 + \sigma^2 v_2 + \dots) \frac{\sigma^{1/2}}{R} \frac{\partial}{\partial \xi} (1 + \sigma \rho_1 + \sigma^2 \rho_2 + \dots) + \right. \\
& \left. + \frac{2c_s (\sigma v_1 + \sigma^2 v_2 + \dots) (1 + \sigma \rho_1 + \sigma^2 \rho_2 + \dots) \sigma^{3/2}}{(R\xi\sigma + R\tau)} \right) + \\
& + c_s^2 (1 + \sigma \rho_1 + \sigma^2 \rho_2 + \dots) (\sigma v_1 + \sigma^2 v_2 + \dots) \left[-\frac{\sigma^{1/2}c_s}{R} \frac{\partial}{\partial \xi} (\sigma v_1 + \sigma^2 v_2 + \dots) + \right. \\
& \left. + \frac{\sigma^{3/2}c_s}{R} \frac{\partial}{\partial \tau} (\sigma v_1 + \sigma^2 v_2 + \dots) + c_s (\sigma v_1 + \sigma^2 v_2 + \dots) \frac{\sigma^{1/2}}{R} \frac{\partial}{\partial \xi} (\sigma v_1 + \sigma^2 v_2 + \dots) \right] = 0 \quad (48)
\end{aligned}$$

Since σ is small we go only up to second order. Therefore (47) and (48) turn into:

$$\begin{aligned}
& \sigma \left(-\frac{\partial v_1}{\partial \xi} + \frac{(\frac{3Mc_s^2}{\rho_0^2} \rho_0 - \frac{2Mc_s^2}{\rho_0}) \rho_0}{\mu_B c_s^2} \frac{\partial \rho_1}{\partial \xi} \right) + \sigma^2 \left[-\frac{\partial v_2}{\partial \xi} + \frac{\partial v_1}{\partial \tau} + v_1 \frac{\partial v_1}{\partial \xi} + \frac{(\frac{3Mc_s^2}{\rho_0^2} \rho_0 - \frac{2Mc_s^2}{\rho_0}) \rho_0}{\mu_B c_s^2} \frac{\partial \rho_2}{\partial \xi} + \right. \\
& \left. \frac{\frac{3Mc_s^2}{\rho_0^2} \rho_0^2}{\mu_B c_s^2} \rho_1 \frac{\partial \rho_1}{\partial \xi} - \frac{(\frac{3Mc_s^2}{\rho_0^2} \rho_0 - \frac{2Mc_s^2}{\rho_0}) \rho_0}{\mu_B} v_1 \frac{\partial \rho_1}{\partial \xi} + \left(\frac{d \frac{g_V^2}{m_V^4} \rho_0}{\mu_B c_s^2 R^2} \right) \frac{\partial^3 \rho_1}{\partial \xi^3} \right] = 0 \quad (49)
\end{aligned}$$

and

$$\sigma \left(-\frac{\partial \rho_1}{\partial \xi} + \frac{\partial v_1}{\partial \xi} \right) + \sigma^2 \left[\frac{\partial v_2}{\partial \xi} + \frac{\partial \rho_1}{\partial \tau} - c_s^2 v_1 \frac{\partial v_1}{\partial \xi} - \frac{\partial \rho_2}{\partial \xi} + v_1 \frac{\partial \rho_1}{\partial \xi} + \rho_1 \frac{\partial v_1}{\partial \xi} + \frac{2}{(\xi \sigma + \tau)} v_1 \right] = 0$$

In the last term of the above expression, since $0 < \sigma < 1$, we shall assume that $\tau > \xi \sigma$ and make the approximation

$$\frac{2}{(\xi \sigma + \tau)} \cong \frac{2}{\tau} \quad (50)$$

and hence:

$$\sigma \left(-\frac{\partial \rho_1}{\partial \xi} + \frac{\partial v_1}{\partial \xi} \right) + \sigma^2 \left(\frac{\partial v_2}{\partial \xi} + \frac{\partial \rho_1}{\partial \tau} - c_s^2 v_1 \frac{\partial v_1}{\partial \xi} - \frac{\partial \rho_2}{\partial \xi} + v_1 \frac{\partial \rho_1}{\partial \xi} + \rho_1 \frac{\partial v_1}{\partial \xi} + \frac{2}{\tau} v_1 \right) = 0 \quad (51)$$

Since the coefficients in the above series are independent of each other we get a set of equations. From the terms proportional to σ in (49) and (51) we find:

$$\rho_1 = v_1 \quad (52)$$

and also

$$\frac{\left(\frac{3Mc_s^2}{\rho_0^2} \rho_0 - \frac{2Mc_s^2}{\rho_0} \right) \rho_0}{\mu_B c_s^2} = 1 \quad (53)$$

and therefore

$$\mu_B = M \quad (54)$$

In fact, in (52) we might have an integration constant. However, as it was shown in [10] for the one dimensional Cartesian case, this would not change the results significantly. For our purposes it is enough to consider (52), keeping in mind that it is only a particular solution of the problem. From the terms proportional to σ^2 in (49) and (51), with the help of (52) and (53), we find:

$$\begin{aligned} -\frac{\partial \rho_1}{\partial \tau} - \rho_1 \frac{\partial \rho_1}{\partial \xi} - 3\rho_1 \frac{\partial \rho_1}{\partial \xi} + c_s^2 \rho_1 \frac{\partial \rho_1}{\partial \xi} - \left(\frac{d \frac{gV^2}{mV^4} \rho_0}{\mu_B c_s^2 R^2} \right) \frac{\partial^3 \rho_1}{\partial \xi^3} = \\ = \frac{\partial \rho_1}{\partial \tau} - c_s^2 \rho_1 \frac{\partial \rho_1}{\partial \xi} + \rho_1 \frac{\partial \rho_1}{\partial \xi} + \rho_1 \frac{\partial \rho_1}{\partial \xi} + \frac{2}{\tau} \rho_1 \end{aligned}$$

which, after a rearrangement of terms and change of variables back to the $r - t$ space, becomes the ‘‘spherical KdV’’ equation:

$$\frac{\partial \hat{\rho}_1}{\partial t} + c_s \frac{\partial \hat{\rho}_1}{\partial r} + (3 - c_s^2) c_s \hat{\rho}_1 \frac{\partial \hat{\rho}_1}{\partial r} + d \left(\frac{gV^2 \rho_0}{2MmV^4 c_s} \right) \frac{\partial^3 \hat{\rho}_1}{\partial r^3} + \frac{\hat{\rho}_1}{t} = 0 \quad (55)$$

for which a suitable initial condition may be:

$$\hat{\rho}_1(r, t_0) = \frac{3(u - c_s)}{c_s} (3 - c_s^2)^{-1} \text{sech}^2 \left[m_V^2 \sqrt{\frac{(u - c_s)c_s M}{2g_V^2 \rho_0}} (r - ut_0) \right] \quad (56)$$

This Gaussian-looking form is motivated by the analytical solution of the KdV equation in one dimensional Cartesian coordinates discussed in [15]. Here, the numbers u, t_0, \dots are parameters without special meaning.

B. Finite temperature

Apart from the trivial replacement of (27) by (16) there is another change when we consider nuclear matter at finite temperature. We do not restrict ourselves to the case where nuclear matter is saturated. Instead, we shall consider the case where there is an equilibrated background with constant density and zero velocity, upon which perturbations propagate, but no saturation. The difference is that with saturation, a system is bound and more stable, whereas in the present case stability is not guaranteed and this system might expand or shrink. In such a situation, perturbations would propagate in an expanding medium and the reference density ρ_0 in (36) might change with time. This is the scenario that we have in heavy ion collisions at RHIC, which we plan to address in the future. Here we consider the simpler case of constant ρ_0 .

Substituting (16) into (13) we obtain:

$$h = \frac{g_V^2}{m_V^2} \rho_B + d \frac{g_V^2}{m_V^4} \vec{\nabla}^2 \rho_B \quad (57)$$

Using the definition of the operators in spherical coordinates we arrive at:

$$\frac{\partial h}{\partial r} = \frac{g_V^2}{m_V^2} \frac{\partial \rho_B}{\partial r} + d \frac{g_V^2}{m_V^4} \frac{\partial^3 \rho_B}{\partial r^3} + d \frac{g_V^2}{m_V^4} \frac{2}{r} \frac{\partial^2 \rho_B}{\partial r^2} - d \frac{g_V^2}{m_V^4} \frac{2}{r^2} \frac{\partial \rho_B}{\partial r} \quad (58)$$

and also

$$\frac{\partial h}{\partial t} = \frac{g_V^2}{m_V^2} \frac{\partial \rho_B}{\partial t} + d \frac{g_V^2}{m_V^4} \frac{\partial}{\partial t} \left(\frac{\partial^2 \rho_B}{\partial r^2} \right) + d \frac{g_V^2}{m_V^4} \frac{2}{r} \frac{\partial}{\partial t} \left(\frac{\partial \rho_B}{\partial r} \right) - d \frac{g_V^2}{m_V^4} \frac{2v}{r^2} \frac{\partial \rho_B}{\partial r} \quad (59)$$

Substituting (58) and (59) into (11) and repeating the steps described in the last section, i.e., introducing dimensionless variables, changing variables to the $\xi - \tau$ space, expanding $\hat{\rho}$ and \hat{v} and collecting the terms proportional to σ and to σ^2 we obtain the following relations from the Euler equation:

$$\sigma \left[- \left(\mu_B + \frac{T_S}{\rho_0} \right) \frac{\partial v_1}{\partial \xi} + \frac{g_V^2}{m_V^2} \frac{\rho_0}{c_s^2} \frac{\partial \rho_1}{\partial \xi} \right] = 0 \quad (60)$$

and

$$\begin{aligned} & \sigma^2 \left[\left(\mu_B + \frac{Ts}{\rho_0} \right) \left(-\frac{\partial v_2}{\partial \xi} + \frac{\partial v_1}{\partial \tau} + v_1 \frac{\partial v_1}{\partial \xi} \right) + \frac{g_V^2 \rho_0}{m_V^2 c_s^2} \rho_1 \frac{\partial \rho_1}{\partial \xi} + \right. \\ & \left. + \frac{g_V^2 \rho_0}{m_V^2 c_s^2} \frac{\partial \rho_2}{\partial \xi} - \mu_B \rho_1 \frac{\partial v_1}{\partial \xi} - \frac{g_V^2}{m_V^2} \rho_0 v_1 \frac{\partial \rho_1}{\partial \xi} + \frac{g_V^2 \rho_0}{m_V^4 c_s^2 R^2} \frac{\partial^3 \rho_1}{\partial \xi^3} \right] = 0 \end{aligned} \quad (61)$$

After some manipulations, the continuity equation (7) is written as:

$$(1 - v^2) \left(\frac{\partial \rho_B}{\partial t} + \rho_B \frac{\partial v}{\partial r} + v \frac{\partial \rho_B}{\partial r} + \frac{2\rho_B v}{r} \right) + v \rho_B \left(\frac{\partial v}{\partial t} + v \frac{\partial v}{\partial r} \right) = 0 \quad (62)$$

which, after the change of variables and expansion yields the following relations:

$$\sigma \left(-\frac{\partial \rho_1}{\partial \xi} + \frac{\partial v_1}{\partial \xi} \right) = 0 \quad (63)$$

and

$$\sigma^2 \left(\frac{\partial v_2}{\partial \xi} + \frac{\partial \rho_1}{\partial \tau} - c_s^2 v_1 \frac{\partial v_1}{\partial \xi} - \frac{\partial \rho_2}{\partial \xi} + v_1 \frac{\partial \rho_1}{\partial \xi} + \rho_1 \frac{\partial v_1}{\partial \xi} + \frac{2}{\tau} v_1 \right) = 0 \quad (64)$$

where in the last term of the above expression we made again the approximation (50). From (60) and (63) we get the relations:

$$\left(\mu_B + \frac{Ts}{\rho_0} \right) = \frac{g_V^2 \rho_0}{m_V^2 c_s^2}$$

and

$$v_1 = \rho_1$$

Substituting these expressions in (61) and (64) and combining the resulting equations we arrive at the finite temperature spherical KdV equation:

$$\frac{\partial \hat{\rho}_1}{\partial t} + c_s \frac{\partial \hat{\rho}_1}{\partial r} + \left(2 - c_s^2 - \frac{\mu_B m_V^2 c_s^2}{2g_V^2 \rho_0} \right) c_s \hat{\rho}_1 \frac{\partial \hat{\rho}_1}{\partial r} + d \left(\frac{c_s}{2m_V^2} \right) \frac{\partial^3 \hat{\rho}_1}{\partial r^3} + \frac{\hat{\rho}_1}{t} = 0 \quad (65)$$

In the numerical studies of this equation we have used an initial condition with the form given by (56) with several choices for the parameters.

C. One dimensional Cartesian coordinates

One dimensional perturbations propagating in cold nuclear matter have been discussed in detail in [15] and [16] and thus we only give here the obtained differential equation:

$$\frac{\partial \hat{\rho}_1}{\partial t} + c_s \frac{\partial \hat{\rho}_1}{\partial x} + (3 - c_s^2) c_s \hat{\rho}_1 \frac{\partial \hat{\rho}_1}{\partial x} + \left(\frac{d g_V^2 \rho_0}{2M m_V^4 c_s} \right) \frac{\partial^3 \hat{\rho}_1}{\partial x^3} = 0 \quad (66)$$

which has the following analytical solution:

$$\hat{\rho}_1(x, t) = \frac{3(u - c_s)}{c_s} (3 - c_s^2)^{-1} \operatorname{sech}^2 \left[\frac{m_V^2}{g_V} \sqrt{\frac{(u - c_s)c_s M}{2d\rho_0}} (x - ut) \right] \quad (67)$$

At finite temperature we replace (27) by (16) and use it directly in (13) without imposing any saturation condition. Everything else is the same as described in the last sections. We arrive at the following equation:

$$\frac{\partial \hat{\rho}_1}{\partial t} + c_s \frac{\partial \hat{\rho}_1}{\partial x} + \left(2 - c_s^2 - \frac{\mu_B m_V^2 c_s^2}{2g_V^2 \rho_0} \right) c_s \hat{\rho}_1 \frac{\partial \hat{\rho}_1}{\partial x} + \left(\frac{d c_s}{2m_V^2} \right) \frac{\partial^3 \hat{\rho}_1}{\partial x^3} = 0 \quad (68)$$

with analytical solution given by:

$$\hat{\rho}_1(x, t) = \frac{3(u - c_s)}{c_s} \left(2 - c_s^2 - \frac{\mu_B m_V^2 c_s^2}{2g_V^2 \rho_0} \right)^{-1} \operatorname{sech}^2 \left[\sqrt{\frac{(u - c_s)m_V^2}{2d c_s}} (x - ut) \right] \quad (69)$$

V. NUMERICAL RESULTS

The numerical solution of non-linear differential equations is not very difficult, but may be very tricky. We benefited from the reading and hints contained in the textbook [28], which has a special section dedicated to solitons.

We start our numerical analysis showing in Fig. 1 the solution of the linear KdV equation at $T = 0$, Eq. (66). In the upper pannel, Fig. 1a), we use the analytical solution Eq. (67) as initial condition. As expected this pulse propagates without dissipation nor dispersion. Any change in the initial condition has noticeable consequences. In Fig. 1b), we follow the evolution of the numerical solution of (66) for an initial pulse given by (67) multiplied by a factor two. As it can be seen, the amplitude grows, the width decreases and a second bumps appears propagating behind the first. In Fig. 1c) we start the evolution with (67) multiplied by a factor seven. Now we have three peaks instead of two. In practical cases, the initial conditions will never be exactly those needed to generate a single pulse. Therefore, in general we expect to see multiple bumps. In Fig. 1 we can also see that perturbations with higher amplitudes propagate faster.

In Fig. 2, we show the equivalent plot for the spherical case. In contrast to the linear case there is a strong damping of the pulse. The dependence on the initial conditions is also strong. The main peak very rapidly loses height and develops secondary bumps.

In Fig. 3 we show for the linear case and for the ‘‘optimal’’ initial condition (67) the evolution of the pulse with time for different temperatures. We can see that, increasing the

temperature the pulses move faster and go farther. The same feature can be observed in the spherical case, as shown in Fig. 4.

Setting $d = 0$ in (14) we recover the standard non-linear Walecka model. In this medium the propagation of density perturbations will be governed by the differential equations (55), (65), (66) and (68) without the terms with the d factor. The absence of the third order derivative terms leads to a lack of stability of the solution. The corresponding differential equations are “shock wave equations”. Out of smooth initial perturbations these equations create shock waves. We can see this process in one dimensional Cartesian coordinates in Fig. 5.

Figure 5a) shows the solution of Eq. (66) with $d = 0$ for the initial condition (56). In Figs. 5b) and 5c) the initial profile has been multiplied by a factor 2 and 10 respectively. In all cases we observe a steepening of the profile until the formation of the shock, followed by the dispersion of the wave. We see that the higher is the initial amplitude, the sooner the wave breaking and dispersion occur. The solutions of (55) with $d = 0$ for three different initial profiles can be seen in Fig. 6, where the three pannels, 6a), 6b) and 6c), show the evolution of the original profile and then the evolution of this profile multiplied by 2 and by 10 respectively. In the spherical case the damping is so strong that wave breaking hardly happens.

In Figure 7 we fix one initial profile and study its time evolution for three different temperatures. Figs. 7a), 7b) and 7c) show the development of a shock wave at $T = 20$ MeV, 70 MeV and 120 MeV respectively. As it can be seen, with increasing temperatures the pulse moves faster and the shock formation and the subsequent dispersive breaking occur sooner. Fig. 8 shows the analogous plot for spherical coordinates.

VI. CONCLUSIONS

From the equations of relativistic hydrodynamics and with an equation of state obtained from a variant of the non-linear Walecka model we have derived a spherical KdV-like equation for perturbations in the baryon density. The coefficients of the differential equation are determined by the microscopic meson exchange dynamics. This is an improvement over our previous study [18]. Moreover we have included temperature effects and solved numerically the resulting differential equations. We have also, for the first time, obtained numerical

solutions for the one dimensional Cartesian case at zero and finite temperature.

The results give a quantitative measure of the dependence of the numerical solutions on the initial conditions. We found that, as expected in non-linear problems, the behavior of the solutions depends very strongly on the initial conditions.

The results presented in Fig. 3 are a first step towards a realistic study of the propagation of a fast leading particle (coming from a jet) crossing hot hadronic matter. They suggest that perturbation may propagate for a relatively long distance preserving features of the initial peak structure. This is even more true at higher temperatures. In contrast, in the spherical case shown in Fig. 4, our results show a strong attenuation, indicating that localized perturbations will not survive for long distances. They will instead release energy to the medium in a more homogeneous way. This behavior may have consequences for astrophysical phenomena and we plan to address this subject in the near future. Switching off the cubic derivative term in the Lagrangian density and recovering the standard non-linear Walecka model, the propagation of initial density pulses generates shock waves, which go through a dispersive breaking. Both the propagation and breaking depend strongly on the properties (height and width) of the initial pulses and on the temperature of the medium. Higher pulses move faster and break earlier. The same effect is observed when we increase the temperature. In contrast, spherical pulses are very insensitive to the initial conditions and to the temperature.

We plan to investigate the consequences of our findings both in the relativistic heavy ion physics and dense stars physics scenarios.

Acknowledgments

We wish to express our gratitude to S. Duarte, F.O. Durães, E. Fraga, T. Kodama, S. Raha, S. Szpigel, Dou Fu-Quan and A. Gammal for numerous suggestions and useful comments and hints. This work was partially financed by the Brazilian funding agencies CAPES, CNPq and FAPESP.

[1] J.Y. Ollitrault, arXiv:0708.2433 [nucl-th];

- [2] U. Heinz, *J. Phys.* **G31**, S717 (2005); for a recent review see P.F. Kolb, U. Heinz, in “Quark Gluon Plasma 3”, Editors: R.C. Hwa and X.-N. Wang, World Scientific, Singapore, (2003) p. 634; nucl-th/0305084.
- [3] R.B. Clare and D. Strottman, *Phys. Rept.* **141**, 177 (1986).
- [4] Y. Hama, T. Kodama and O. Socolowski Jr., *Braz. J. Phys.* **35**, 24 (2005); Y. Hama and F.S. Navarra, *Phys. Lett.* **B129**, 251 (1983); *Z. Phys.* **C53**, 501 (1992).
- [5] K. H. Ackermann *et al.* [STAR Collaboration], *Phys. Rev. Lett.* **86**, 402 (2001); P. Huovinen, P. F. Kolb, U. W. Heinz, P. V. Ruuskanen and S. A. Voloshin, *Phys. Lett.* **B503**, 58 (2001); S. S. Adler *et al.* [PHENIX Collaboration], *Phys. Rev. Lett.* **91**, 182301 (2003).
- [6] L. M. Satarov, H. Stoecker and I. N. Mishustin, *Phys. Lett.* **B627**, 64 (2005); T. Renk and J. Ruppert, *Phys. Rev.* **C73**, 011901 (2006); T. Renk and J. Ruppert, *Phys. Lett.* **B646**, 19 (2007).
- [7] S. S. Adler *et al.* [PHENIX Collaboration], *Phys. Rev. Lett.* **97**, 052301 (2006).
- [8] J. Adams *et al.*, STAR Collab. *Phys. Rev. Lett.* **95**, 152301 (2005).
- [9] G.N. Fowler, S. Raha, N. Stelte and R.M. Weiner, *Phys. Lett.* **B115**, 286 (1982); S. Raha and R.M. Weiner, *Phys. Rev. Lett.* **50**, 407 (1983); E.F. Hefter, S. Raha and R.M. Weiner, *Phys. Rev.* **C32**, 2201 (1985).
- [10] S. Raha, K. Wehrberger and R.M. Weiner, *Nucl. Phys.* **A433**, 427 (1984).
- [11] A.Y. Abul-Magd, I. El-Taher and F.M. Khaliel, *Phys. Rev.* **C45**, 448 (1992).
- [12] G.A. Lalazissis, J. König and P. Ring, *Phys. Rev.* **C55**, 540 (1997).
- [13] R.J. Furnstahl, *Lect. Notes Phys.* **641**, 1 (2004); B.D. Serot, *Int. J. Mod. Phys.* **A19S1**, 107 (2004) and references therein.
- [14] B.D. Serot and J.D. Walecka, *Advances in Nuclear Physics* **16**, 1 (1986).
- [15] D.A. Fogaça and F.S. Navarra, *Phys. Lett.* **B639**, 629 (2006).
- [16] D.A. Fogaça and F.S. Navarra, *Phys. Lett.* **B645**, 408 (2007).
- [17] D.A. Fogaça and F.S. Navarra, *Nucl. Phys.* **A790**, 619c (2007).
- [18] D.A. Fogaça and F.S. Navarra, *Int. J. Mod. Phys.* **E 16**, 3019 (2007).
- [19] J.-K. Xue, *Phys. Lett.* **A322**, 225 (2004).
- [20] L.K. Pu, D. Fu-Quan, S. Jian-An, D. Wen-Shan, S. Yu-Ren, *Chinese Phys.* **14**, 33 (2005); *Chinese Phys. Lett.* **18**, 1088 (2001).
- [21] S. Weinberg, “Gravitation and Cosmology”, New York: Wiley, 1972.

- [22] L. Landau and E. Lifchitz, “Fluid Mechanics”, Pergamon Press, Oxford, (1987).
- [23] H.-T. Elze, Y. Hama, T. Kodama, M. Makler and J. Rafelski, *J. Phys. G: Nucl. Part. Phys.* **25**, 1935 (1999).
- [24] R. Reif, “Fundamentals of statistical and thermal physics”, New York: McGraw-Hill, 1965.
- [25] For a recent example see M. Chiapparini, M. E. Bracco, A. Delfino, M. Malheiro, D. P. Menezes and C. Providência, arXiv:0711.3631 [hep-ph] and references therein.
- [26] N. Sasaki, O. Miyamura, S. Muroya, C. Nonaka, *Europhys. Lett.* **54**, 38 (2001); *Phys. Rev.* **C62**, 011901 (2000).
- [27] R.C. Davidson, “Methods in Nonlinear Plasma Theory”, Academic Press, New York and London, 1972.
- [28] R.H. Landau and M.J. Paez Mejia, “Computational physics: problem solving with computers”, New York: John Wiley, 1997.

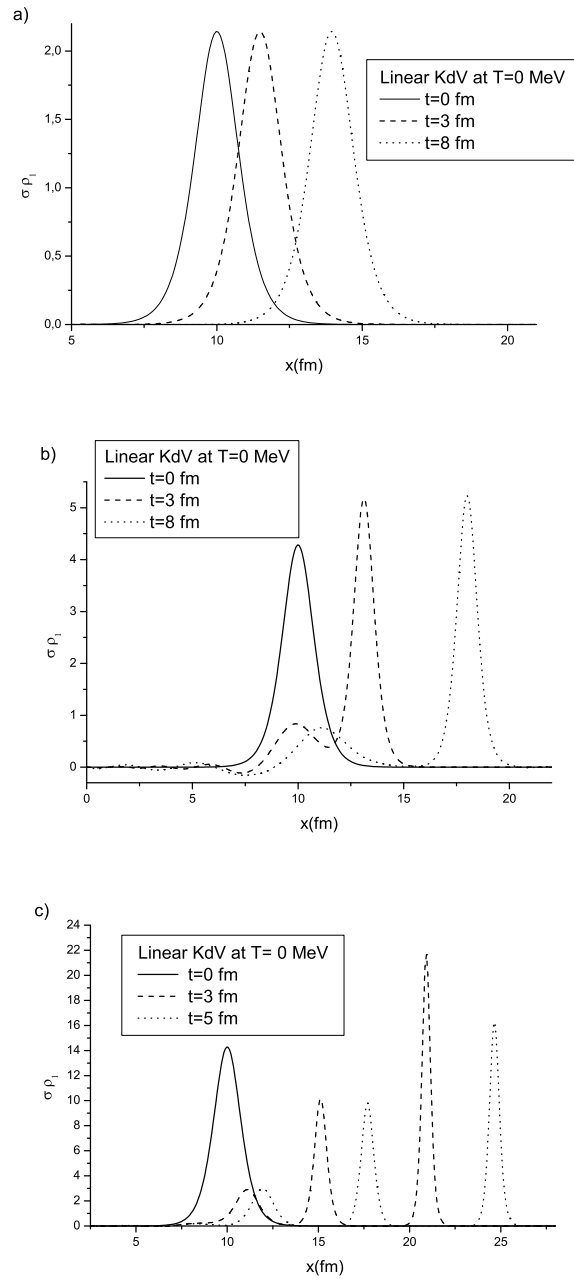


FIG. 1: Time evolution of a density perturbation in arbitrary units in one dimensional Cartesian coordinates. The upper panel shows the evolution of the analytic solution of the KdV equation. In the lower panels we show the evolution of the analytic solution multiplied by a factor 2 and 7 respectively.

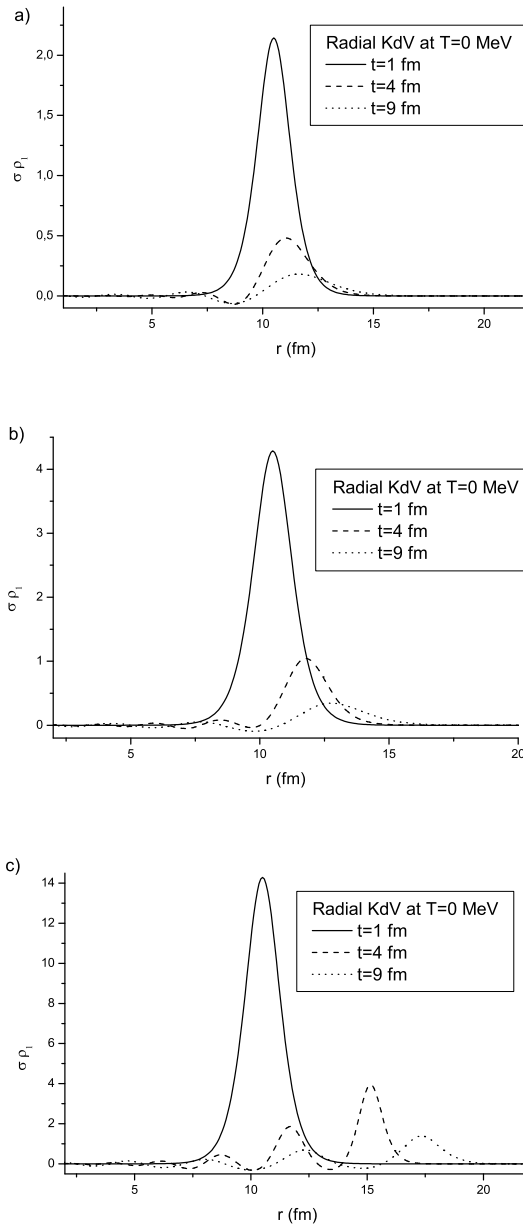


FIG. 2: The same as Figure 1 for spherical coordinates.

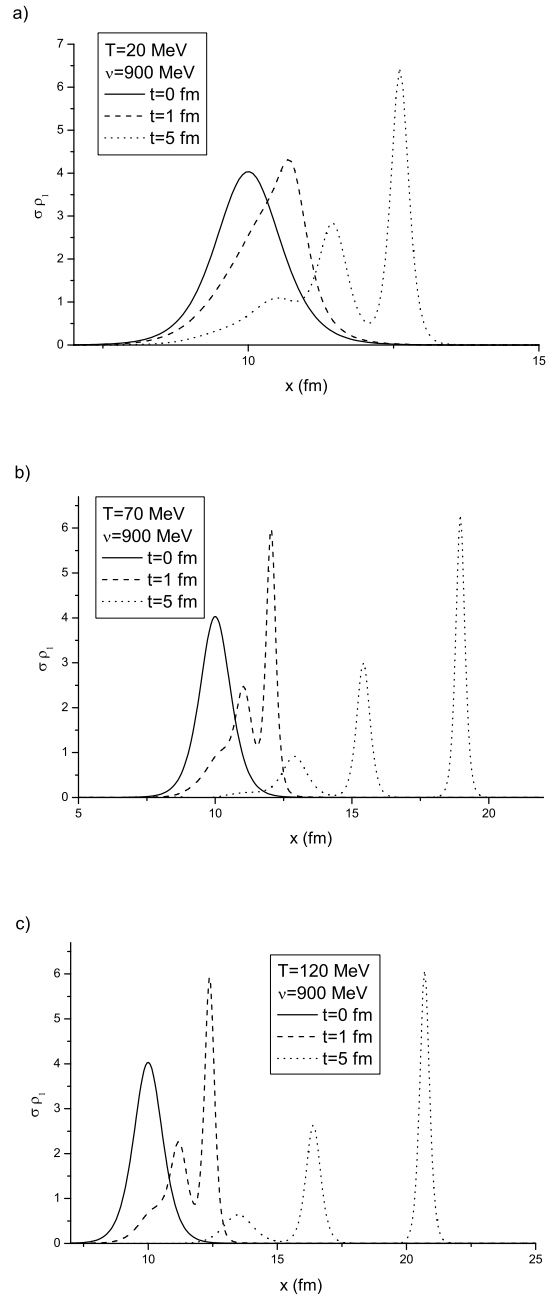


FIG. 3: Time evolution of density perturbations in one dimensional Cartesian coordinates as a function of the temperature. The panels show calculations with temperatures $T = 20, 70$ and 120 MeV respectively.

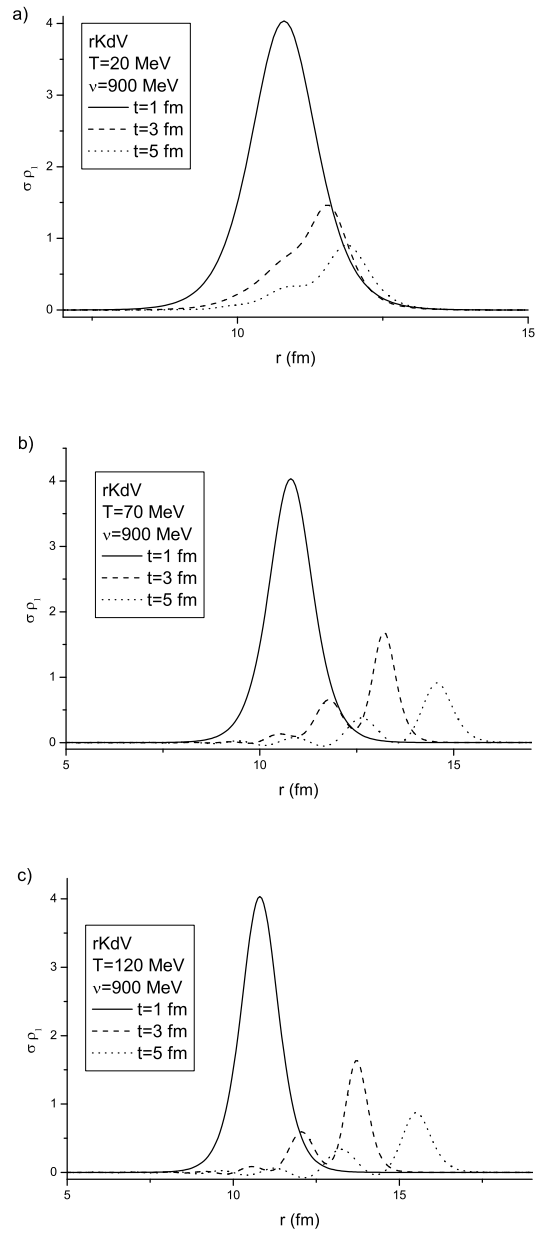


FIG. 4: The same as Figure 3 for one dimensional spherical coordinates

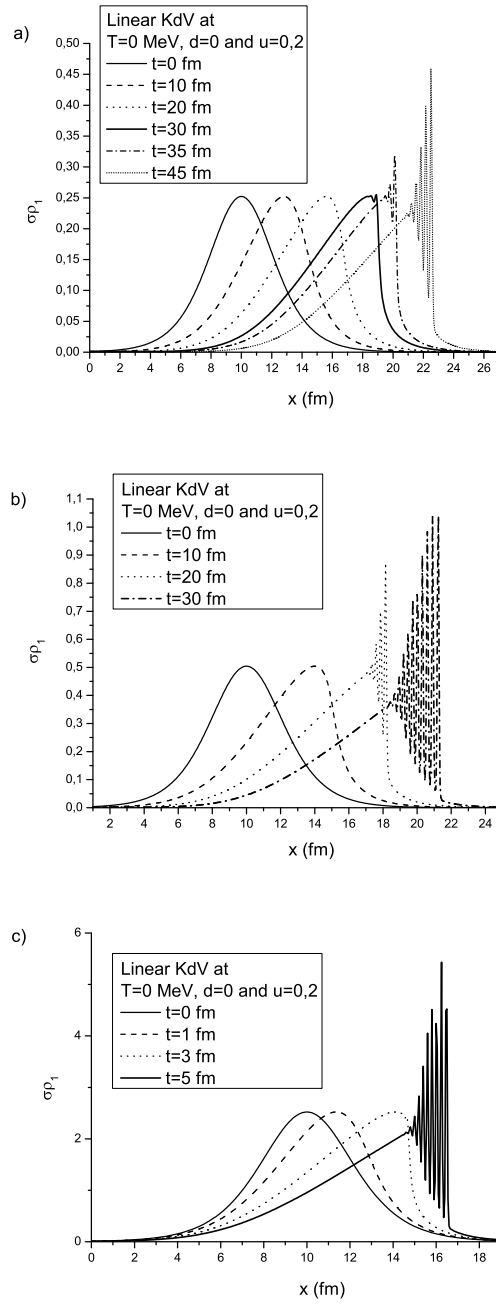


FIG. 5: Shock wave formation in one dimensional Cartesian coordinates. a) Initial profile with height 0.25 (arbitrary units); b) with height 0.50; c) with height 2.5.

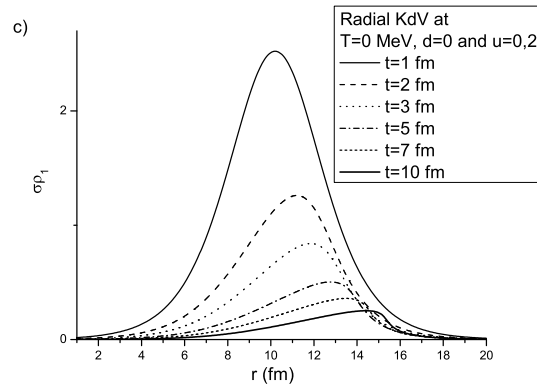
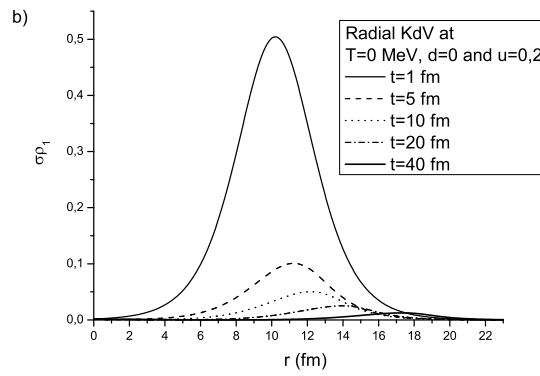
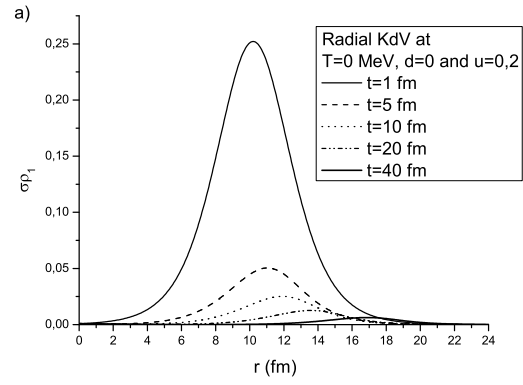


FIG. 6: The same as Figure 5 in one dimensional spherical coordinates

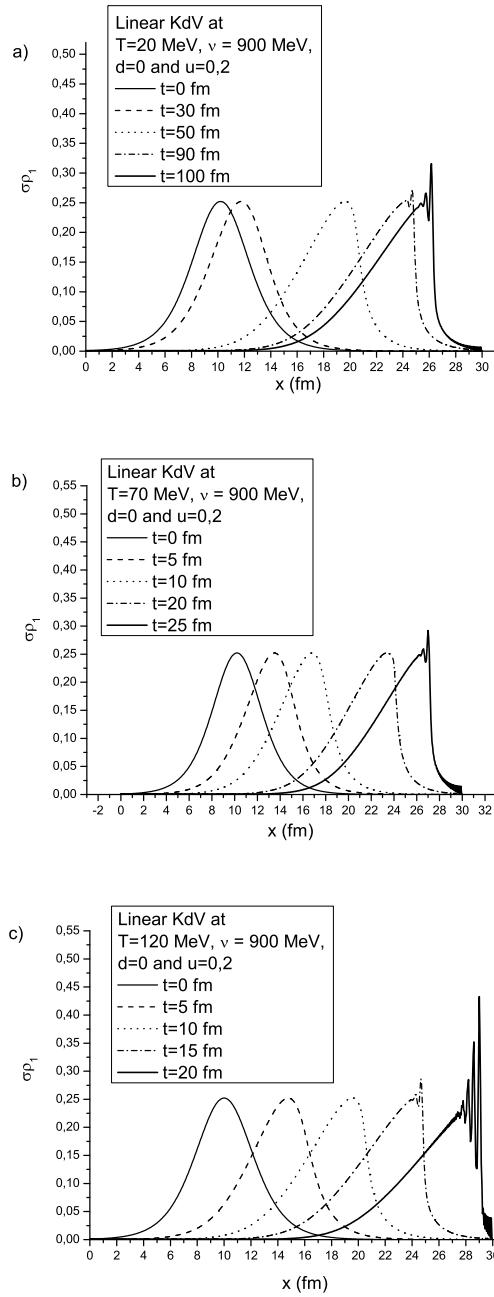


FIG. 7: Shock wave formation in one dimensional Cartesian coordinates for different temperatures.

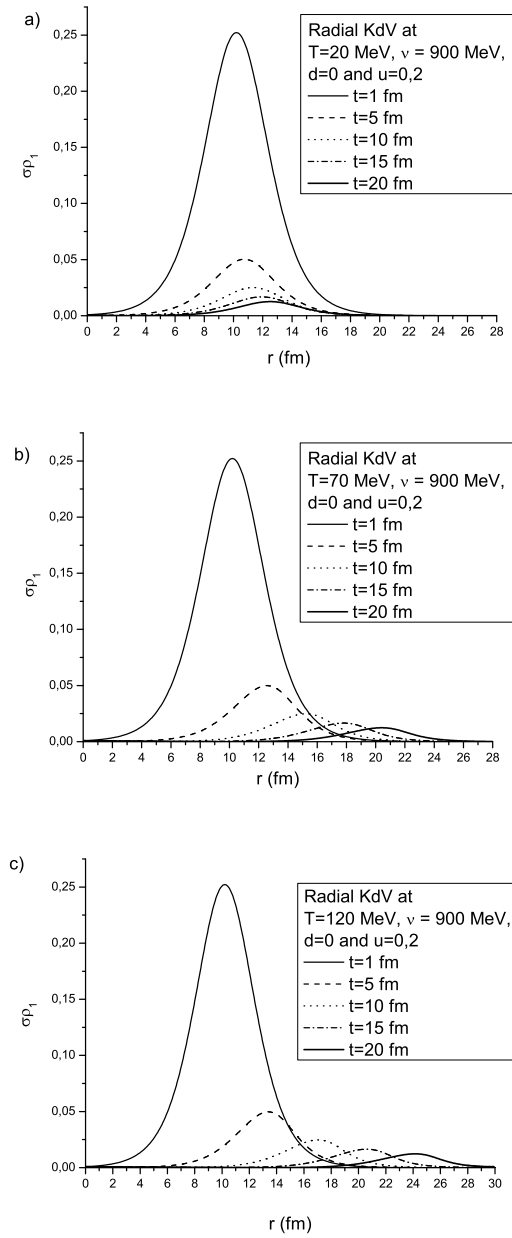


FIG. 8: The saem as Figure 7 for one dimensional spherical coordinates.